2nd URSI AT-RASC, Gran Canaria, 28 May – 1 June 2018

Overview of possibilities of spatial signal processing in an inhomogeneous medium based on integral representation of wave field as double weighted Fourier transform (DWFT)

M. Tinin
Irkutsk State University, Irkutsk, Russia, 664003, http://www.isu.ru

Abstract

The report reviews the results obtained with the method of double weighted Fourier transform and possibilities of this transform in spatial signal processing. We give examples of this processing for eliminating amplitude scintillations, increasing resolution, and eliminating ionospheric errors in GNSS measurements.

1. Introduction

Asymptotic methods are widely used in the theory of wave propagation in inhomogeneous media. Since the commonly used methods are applicable only in certain regions and under certain conditions, there arises the need for "uniform" asymptotic expressions connecting these non-uniform asymptotic expressions. Moreover, the ratio of wave parameters (wavelength, Fresnel radius, etc.) to the scale of irregularity is often adopted as a small parameter in the asymptotic methods. Since many inhomogeneous media are multiscale, such "uniform" asymptotic expressions are necessary both for direct and inverse problems of radio wave propagation in inhomogeneous media. The uniform asymptotic expressions describing effects of irregularities of different scales in various regions (illuminated, caustic, and caustic shadow) quite often have the form of an integral representation. The inverse of this integral asymptotic representation can sometimes be used as an algorithm for spatial signal processing in a multiscale inhomogeneous medium. Here, we examine possibilities of the integral representation, obtained by the DWFT method, for spatial processing.

2. First DWFT approximation

Let a source and a receiver be at the respective points $\mathbf{r}_0 = (z_0, x_0, y_0) = (z_0, \boldsymbol{\rho}_0)$ and $\mathbf{r} = (z_t, x, y) = (z_t, \boldsymbol{\rho})$. Assume that the scale of irregularity l_ε of permittivity $\varepsilon(\mathbf{r}) = 1 + \tilde{\varepsilon}(\mathbf{r})$ exceeds the wavelength λ, i.e. $kl_\varepsilon = 2\pi l_\varepsilon / \lambda >> 1$, and take into account that in this case the forward scattering is predominant. Then the solution of the wave equation for the wave field $U(\mathbf{r}, \mathbf{r}_0)$ reduces to the solution of the parabolic equation. Solving this equation using the DWFT method, we get [1-3]:

$$U(\boldsymbol{\rho}, \boldsymbol{\rho}_0) = -\frac{k^2 A_0}{4\pi^3 Z^3} \exp\left[ik\left(Z + \frac{(\boldsymbol{\rho} + \boldsymbol{\rho}_0)^2}{2Z}\right)\right] \times \int_{-\infty}^{\infty}\int_{-\infty}^{\infty} d^2\xi d^2\xi_0 \exp\left\{ik\left[\frac{2}{Z}(\boldsymbol{\xi}\boldsymbol{\xi}_0 - \boldsymbol{\xi}\boldsymbol{\rho}_0 - \boldsymbol{\xi}_0\boldsymbol{\rho}) + \Phi\right]\right\}, \quad (1)$$

$$\Phi(\boldsymbol{\xi}, \boldsymbol{\xi}_0) = \frac{1}{2}\int_{z0}^{zt} \tilde{\varepsilon}\left[\frac{\boldsymbol{\xi}}{Z}(z' - z_0) + \frac{\boldsymbol{\xi}_0}{Z}(z_t - z'), z'\right] dz' , \quad (2)$$

$Z = z_t - z_0$, A_0 is the incident wave amplitude.
Note that the integrand in (1) in the first approximation does not contain amplitude variations caused by irregularities.

If $l_{\varepsilon\min}$ is the minimum size of irregularities, then, if the condition $a_{fr}(z_0, z_t, z') = \sqrt{(z' - z_0)(z_t - z')/(kZ)} << l_{\varepsilon\min}$ holds for all z' within the inhomogeneous region, the fourfold integral in (1) is calculated by the stationary phase method and (1) reduces to the geometrical optics (GO) approximation [1-3]. When this condition does not hold, for weak phase fluctuations (1) yields results of the Rytov method [1-2], and for small extent of the inhomogeneous medium (1) yields results of the phase screen method [3-4]. Thus, representation (1) accounts for both Fresnel diffraction effects at weak phase fluctuations and strong fluctuations associated with multipath propagation and caustics.

3. Spatial processing based on DWFT

Besides the lack of amplitude variations in partial waves, integrand (1) does not contain coordinates $\boldsymbol{\rho}_0$ and $\boldsymbol{\rho}$ in Φ. Therefore, the inverse DWFT applied to (1) gives [1-3]:

$$L[U(\boldsymbol{\rho}, \boldsymbol{\rho}_0)] = \int_{-\infty}^{\infty}\int_{-\infty}^{\infty} d^2\rho d^2\rho_0 U(\boldsymbol{\rho}, \boldsymbol{\rho}_0) \times \exp\left\{-ik\left[Z + \frac{(\boldsymbol{\rho} + \boldsymbol{\rho}_0)^2}{2Z}\right] + i\frac{2k}{Z}[\boldsymbol{\rho}^*\boldsymbol{\rho}_0 + \boldsymbol{\rho}_0^*\boldsymbol{\rho}]\right\} \quad (3)$$
$$= -A_0 0,25\pi Z k^{-2} \exp\left\{ik\left[2\frac{\boldsymbol{\rho}^*\boldsymbol{\rho}_0^*}{Z} + \Phi(\boldsymbol{\rho}^*, \boldsymbol{\rho}_0^*)\right]\right\}.$$

Expression (3) allows us to obtain linear integral (2) from measurement results $U(\boldsymbol{\rho},\boldsymbol{\rho}_0)$. Linear integral (2) is used when reconstructing the distribution $\tilde{\varepsilon}(\mathbf{r})$ in methods for diagnosing inhomogeneous media, for example in tomography. Expression (2) is analogous to the eikonal in the GO approximation, which is applicable, when the transverse irregularities size l_ε larger than the Fresnel radius a_{fr}. Spatial processing (3) makes it possible to study irregularities with $l_\varepsilon < a_{fr}$, i.e. to achieve the super-Fresnel resolution [1–3, 5].

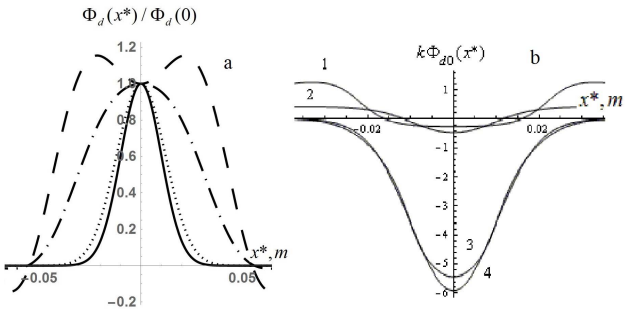

Figure 1. Behavior of normalized linear integrals: (a) for a weak perturbation for sizes of receiving and transmitting apertures $D = D_0$ equal to 2 cm (dashed line), 3 cm (dash-dotted line), 10 cm (dotted line), and ideal projection (solid line);) (b) for a strong perturbation for $D = D_0$ equal to 0 cm (1), 3 cm (2), 15 cm (3), and ideal projection (4).

Figure 1a shows results of simulation [2] of processing (3) for weak phase perturbations, where $\Phi_d(x^*) = \Phi(\boldsymbol{\rho}^*, \boldsymbol{\rho}_0^*)\big|_{y^*=y_0^*=0}$, for a Gaussian irregularity $\tilde{\varepsilon}(\boldsymbol{\rho},z) = \varepsilon_m \exp\left\{-\left[\boldsymbol{\rho}^2+z^2\right]/\left(2l^2\right)\right\}$, with $\varepsilon_m = -0.01$, $l = 1\,\text{cm}$, $z = 3\,\text{m}$, $z_0 = -3\,\text{m}$, $\lambda = 2\,\text{mm}$. In this case, the Fresnel radius at the location of the irregularity is 5.4 cm. As the field under processing the authors [2] use the solution of the problem in the first Rytov approximation. They take the finiteness of processing regions into account by introducing weight functions into the kernel of the integral operator L $V_{tr}(\boldsymbol{\rho}_0) = \exp\left\{-\boldsymbol{\rho}_0^2/\left(2D^2\right)\right\}$ in the transmitting plane and $V_{rc}(\boldsymbol{\rho}) = V_{tr}(\boldsymbol{\rho})$ in the receiving plane.

Resolution also increases through inversion (3) during strong phase variations [3]. Figure 1b presents results of simulation of inversion (3) for the same conditions as in Figure 1a, but with larger irregularity amplitude $\varepsilon_{\varepsilon_m} = -0.15$. While in this case phase variations are sufficiently high, spatial processing (3) with $D = D_0 = 15\,\text{cm}$ (3 line) makes it possible to construct an irregularity profile.

Referring to Figure 1, with small sizes of receiving and transmitting apertures there are oscillations, associated with diffraction effects, in the dependence of the linear integral on the transverse coordinate. With increasing aperture dimensions, these oscillations disappear, and the dependence $\Phi_d(x^*)$ narrows, i.e. resolution increases.

Figure 2 presents results of the study [5] of the dependence of this resolution on sizes of processing areas for three Gaussian irregularities, i.e. with

$$\tilde{\varepsilon}(x,z) = \sum_{i=1}^{3} \varepsilon_{mi} \exp\left\{-\left[(x-x_{\mathbf{m}i})^2 + (z-z_{mi})^2\right]/2l_i^2\right\}$$

for $\lambda = 1{,}85m$, $l_1 = l_2 = l_3 = 90m$, $\varepsilon_1 = \varepsilon_2 = \varepsilon_3 = -0.0025$, $x_{m1} = -350m$, $x_{m2} = 0$, $x_{m3} = -350m$, $z_t = -400km$, $z_0 = 400km$, $z_{m1} = z_{m2} = z_{m3} = 0$ and various $D = D_0$

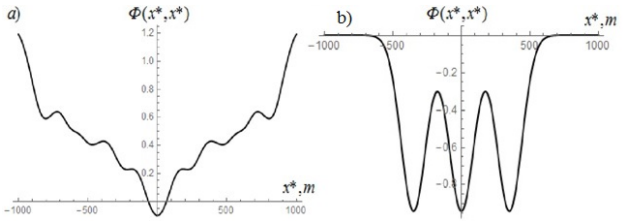

Figure 2. Phase variations for three Gaussian irregularities at $D = D_0 = 50\,\text{m}$ (a), $D = D_0 = 5000\,\text{m}$ (b).

Inversion (3) can be used to explore inhomogeneous media under multipath conditions [6]. Moreover, (3) can be used for a focusing irregularity with sizes smaller than the Fresnel radius of an incident wave. Figure 3 presents results of the simulation [6] for the same conditions as in Figure 1, but with $l = 2\,\text{cm}$ and a positive perturbation $\varepsilon_m = 0.1 > 0$. A possibility is also shown of diagnostics of such irregularity.

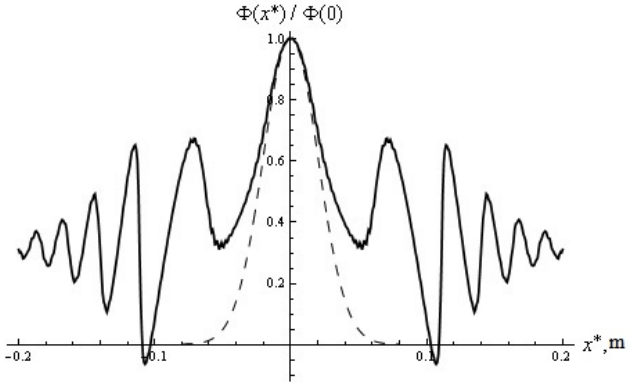

Figure 3. Normalized increment of phase without processing (solid line) and after processing by DWFT (dashed line) for a focusing irregularity with sizes smaller than the Fresnel radius

Note that, as inferred from (3), the DWFT spatial processing can help to eliminate amplitude fluctuations. The results of the simulation of a decrease in the

scintillation index in view of the boundedness of processing regions are given in [7]. In this case, contrary to conventional methods of eliminating fading through space diversity schemes, the authors [7] perform coherent signal processing over two planes.

4. Spatial processing with irregularities being at a great distance from transmitter and observer

When employing the DWFT model to improve resolution of diagnostic tools for inhomogeneous media and to eliminate scintillations, we should process the field over two planes – receiving and transmitting. Such a procedure is not always possible in ionospheric and space plasma studies. However, for a remote irregularity, DWFT (1) can be transformed to an integral over a single plane [4].

To do this, let us turn in (1) to new variables $\boldsymbol{\xi}_0 = \boldsymbol{\rho}_b + \mathbf{p}_s(z_b - z_0)$, $\boldsymbol{\xi} = \boldsymbol{\rho}_b - \mathbf{p}_s(z_t - z_b)$, where $z = z_b$ is a virtual plane (screen) in the vicinity of a remote volume with irregularities. In this case, we can asymptotically calculate the integral over $\boldsymbol{\rho}_s$ and get [4]:

$$U(\boldsymbol{\rho},\boldsymbol{\rho}_0) = \frac{iA_0 k}{8\pi^2}\int_{-\infty}^{\infty}\frac{d^2\rho_b}{(z_t - z_b)(z_b - z_0)}\exp\Big[ik \times\left(Z + \frac{(\boldsymbol{\rho}-\boldsymbol{\rho}_b)^2}{2(z_t - z_b)} + \frac{(\boldsymbol{\rho}_b - \boldsymbol{\rho}_0)^2}{2(z_b - z_0)} + \varphi_b(\boldsymbol{\rho}_b)\right)\Big], \quad (4)$$

$$\varphi_b(\boldsymbol{\rho}_b) = 1/2\int_{z_0}^{z_t}\tilde{\varepsilon}\left[\boldsymbol{\rho}_b + \mathbf{p}_{sc}(z_b - z'), z'\right]dz', \quad (5)$$

$$\mathbf{p}_{sc}(\boldsymbol{\rho}_b) = 0.5\left[(\boldsymbol{\rho}_b - \boldsymbol{\rho})/(z_t - z_b) - (\boldsymbol{\rho}_b - \boldsymbol{\rho}_0)/(z_b - z_0)\right]. \quad (6)$$

In fact, we obtain generalization of the phase screen method contrary to which a small but finite extent of an inhomogeneous medium is taken into account here. Besides, the virtual screen $z = z_b$ can be located anywhere, not just at the output of the inhomogeneous medium.

Now inversion (3) takes the form of Fresnel inversion [4]:

$$\hat{U}(\boldsymbol{\rho}^*,\boldsymbol{\rho}_0) = L_b[U(\boldsymbol{\rho},\boldsymbol{\rho}_0)] = C_0\int_{-\infty}^{\infty} d^2\rho U(\boldsymbol{\rho},\boldsymbol{\rho}_0)\exp\left\{-ik\frac{(\boldsymbol{\rho}^*-\boldsymbol{\rho})^2}{2(z_t - z_b)} - ikZ\right\}. \quad (7)$$

Substituting (4) in (7) yields

$$\hat{U}(\boldsymbol{\rho}^*,\boldsymbol{\rho}_0) \approx \frac{iC_0 A_0(z_t - z_b)}{2k(z_b - z_0)} \times\exp\left\{ik\frac{(\boldsymbol{\rho}^*-\boldsymbol{\rho}_0)^2}{2(z_b - z_0)} + \frac{ik}{2}\int_{z_0}^{z_t}\tilde{\varepsilon}\left[\mathbf{S}_0(z'), z'\right]dz'\right\}, \quad (8)$$

$$\mathbf{S}_0(z') = \boldsymbol{\rho}^*(z' - z_0)/(z_b - z_0) + \boldsymbol{\rho}_0(z_b - z')/(z_b - z_0). \quad (9)$$

As seen from (8)–(9), inversion (7) gives linear integrals along straight lines passing through points $\{\boldsymbol{\rho}^*, z_b\}$ and $\{\boldsymbol{\rho}_0, z_0\}$. With (4)–(9), the DWFT method allows us to explore possibilities of Fresnel inversion for diagnosing inhomogeneous media and to obtain criteria for selecting the position of the virtual screen [4].

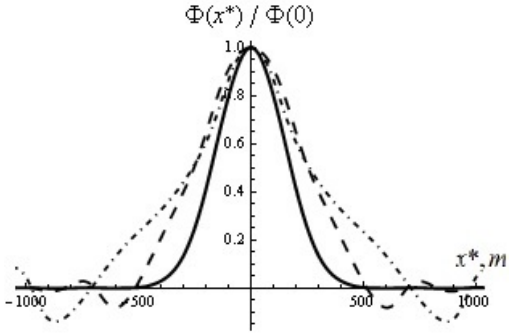

Figure 4. Normalized phase increment after spatial processing (7) when a Gaussian irregularity is located at the origin, for $z_b = 0$ m (solid line), $z_b = 100$ km (dashed line), $z_b = 250$ km (dash-dotted line)

Results of the simulation of the normalized increments of phase and level for weak and strong phase fluctuations are reported in [4] and [8], correspondingly. Figure 4, taken from [8], shows the normalized phase increment for different values of z_b and the following values of other parameters: $x_m = z_m = 0$, $\varepsilon_m = -0.07$, $l = 150$ m , $z_t = -300$ km , $z_0 = 300$ km , $\lambda = 1.5$ m . In this case, the Fresnel radius $a_F \approx 1.12$ km exceeds dimensions of the irregularity.

Let us call attention to the fact that the best resolution is achieved when the virtual screen is placed in the center of the irregularity [4, 8], and not at the output from the inhomogeneous region, as is customary in the phase screen theory. In this case, the decrease in amplitude variations [4, 8] can be used to eliminate signal intensity fluctuations with the aid of Fresnel processing (7), which, unlike (3), is performed at one end of the path.

Elimination of diffraction effects by Fresnel inversion proves important in precision GNSS measurements. The presence of ionospheric irregularities with scales less than the Fresnel radius causes diffraction errors in multi-frequency GNSS [9-11]. In [9–11], the Fresnel inversion of two-frequency and three-frequency GNSS measurements has been studied. Figure 5, taken from [11], presents the results of calculations of processing (7) for the elevation angle of 20° for the mean error (a) and for the standard errors (b) of first (solid lines) and third (dashed line) orders for two-frequency (thin lines) and three-frequency (thick lines) measurements at GPS frequencies. As an ionospheric layer model we take the Chapman layer with the following parameters: the height

is 320 km, the critical frequency is $15\times10^6\,Hz$, the characteristic scale of the layer is 70 km. The turbulent spectrum of plasma irregularities is specified by inner (70 m) and outer (20 km) scales and by the root-mean-square deviation equal to 7% of the background electron density.

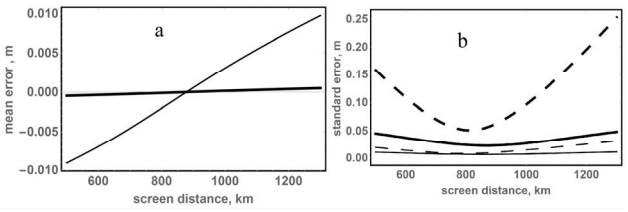

Figure 5. Elimination of diffraction effects from errors of the first (solid lines) and third (dashed line) orders during two-frequency (thin lines) and three-frequency (thick lines) GNSS measurements in the mean error (a) and in the standard error (b).

Figure 5 demonstrates the possibilities of eliminating the diffraction error. To improve measurement accuracy, the position of the virtual screen in processing (7) can be chosen from the condition of minimum error variance or of amplitude fluctuations after inversion [9-11].

5. Conclusion

We have reviewed a number of papers to demonstrate some possibilities of integral representations on the basis of DWFT in spatial signal processing to increase resolution in diagnostics, to reduce amplitude fluctuations, and to eliminate diffraction effects from GNSS measurements. There may be a wider range of applications: to decrease intensity fluctuations during energy transfer from solar satellites, to use the spatial signal processing (7) in the wavefront inversion method and in other methods of adapting optical and radio systems, etc. However, for the proposed spatial processing algorithms to be applied in practice, it is necessary to solve the problems of their robustness and space discretization.

6. Acknowledgments

This work was supported by a project part of the Government Assignment for Scientific Research from the Ministry of Education and Science, Russia (No. 3.903.2017/4.6). I am very grateful to O.A. Kulish for her assistance in preparing the English version of the manuscript.

7. References

1. Yu. A. Kravtsov, and M.V. Tinin, “Representation of a wave field in a randomly inhomogeneous medium in the form of the double-weighted Fourier transform,” *Radio Sci*., **35**, (6), 2000, pp. 1315-1322.

2. M.V. Tinin, and Yu. A. Kravtsov, “Super – Fresnel resolution of plasma inhomogeneities by electromagnetic sounding”, *Plasma Physics and Controlled Fusion*, **50**, 035010, 2008.

3. Yu.A. Kravtsov, M.V. Tinin, and S.I. Knizhnin, “Diffraction Tomography of Inhomogeneous Medium in the Presence of Strong Phase Variations” *Journal of Communications Technology and Electronics*, **56**(7), 2011, pp. 831–837.

4. M.V. Tinin, “Integral representation of the field of the wave propagating in a medium with large-scale irregularities,” Radiophysics and Quantum Electronics, 55(6), 2012, pp. 391-398, doi:10.1007/s11141-012-9376-y

5. A.D. Tkachev, S.I. Knizhin, and M.V. Tinin, “Influence of apertures of receiving –transmitting system on DWFT spatial field processing in diagnostics of inhomogeneous plasma,” *Proceedings of SPIE*, **10466**, 1046611. – doi: 10.1117/12.2285160 8.

6. M.V.Tinin, and S.I.Knizhin, “Eliminating the effects of multipath signal propagation in a smoothly inhomogeneous medium,” *Radiophysics and Quantum Electronics*, **56**(7) , 2013, pp. 413 – 421.

7. M.V. Tinin, and B.C. Kim, “Suppressing amplitude fluctuations of the wave propagating in a randomly inhomogeneous medium,” *Waves in Random and Complex Media*, **21**(4), 2011, pp. 645-656.

8. M.V. Tinin, S.I. Knizhin, “The using of the quasi-optimal field processing for the diagnostics of the near-Earth plasma,” *Izvestiya Irkutskogo Gosudarstvennogo Universiteta (the Bulletin of Irkutsk State University)*, **6**(2). 2013, pp. 175-186 (in Russian).

9. M.V. Tinin, “Eliminating diffraction effects during multi-frequency correction in Global Navigation Satellite Systems,” *Journal of Geodesy,* **89,** 2015, pp. 491–503.

10. M.V. Tinin, “Influence of Ionospheric Irregularities on GNSS Remote Sensing,” *Advances in Meteorology,* **2015,** 2015, Article ID 532015. (10 pages).

11. M.V. Tinin, “Double weighted Fourier transform method in the theory of radiowave propagation in inhomogeneous media: prospects for the development and use of space-time signal processing,” *Proceedings of the XXIV National Conference on Radiowave Propagation*. Irkutsk, 2014, Vol. 4, pp. 175–178 (in Russian). http://rrv.iszf.irk.ru/